Silicon-Tungsten Calorimeter for the Forward Direction in the PHENIX Experiment at RHIC

***Abstract*— The PHENIX detector at RHIC has been designed to study hadronic and leptonic signatures of the Quark Gluon Plasma in heavy ion collisions and spin dependent structure functions in polarized proton collisions. The baseline detector measures muons in two muon spectrometers located forward and backward of mid-rapidity, and measures hadrons, electrons, and photons in two central spectrometer arms, each of which covers 90° in azimuth and 0.35 units of rapidity. Further progress requires extending rapidity coverage for hadronic and electromagnetic signatures by upgrading the functionality of the PHENIX muon spectrometers to include photon and jet measurement capabilities. Tungsten calorimeters with silicon pixel readout and fine transverse and longitudinal segmentation are proposed to attain this goal. The use of such a design provides the highest density and finest granularity possible in a calorimeter.**

***Index Terms*—Calorimeter, forward spectrometer, mechanical design, analog and digital readout electronics, triggering .**

I.INTRODUCTION

The PHENIX [1,2] detector (Fig.1) is designed to perform a broad study of nucleus-nucleus (A-A), proton or deuteron nucleus (p-A or d-A), and proton-proton (p-p) collisions to investigate nuclear matter under extreme conditions and spin dependent structure functions. The needs of the heavy-ion and polarized-proton programs have produced a detector with unparalleled capabilities. PHENIX measures electrons muons, photons, and hadrons with excellent energy and momentum resolution. The PHENIX detector utilizes global detectors to characterize the collisions, a pair of central spectrometers at mid rapidity to measure electrons, hadrons, and photons, and a pair of forward spectrometers to measure muons. Each spectrometer has a geometric acceptance of about one steradian and excellent particle identification.

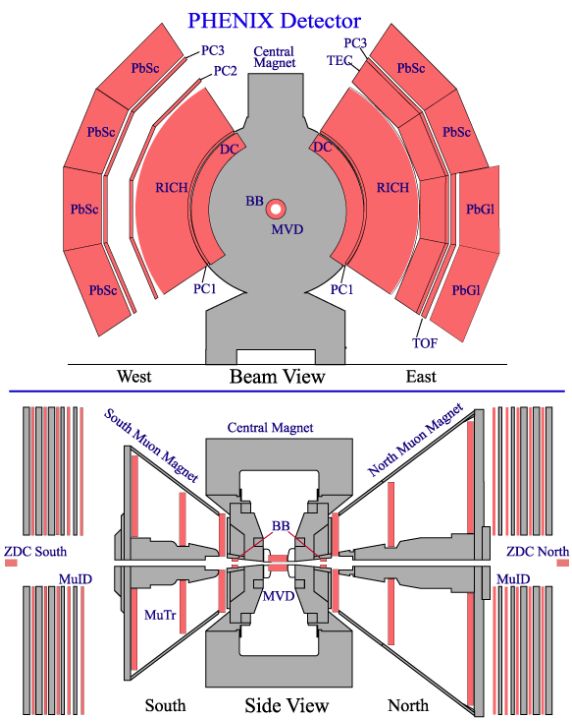

Fig. 1. A beam view (top) and side view (bottom) of the PHENIX detector in its most recent configuration. MVD - Multiplicity Vertex Detector; BB-Beam-Beam trigger counters; DC-Drift Chambers; RICH - ring imaging Cherenkov counters; PC-Pad Chambers; TEC - Time Expansion Chambers; PbSc/PbGl – Electromagnetic Calorimeters; MuTr/MuId -Muon Tracking and Muon Identification; ZDC - Zero Degree Calorimeters. There is an axial magnetic field in the central regions; the muon magnets produce a radial magnetic field.

The proposed forward spectrometer upgrade will introduce new detector elements in the forward direction which will result in a ten-fold increase in rapidity coverage for charged hadrons and photons. This upgrade will provide us the access to the physics observables that are to date not accessible to PHENIX or available only indirectly with very limited accuracy. Forward production of inclusive jets, direct photons or Drell-Yan pairs at large xF in nucleon-ion collisions at RHIC will provide a new window for the observation of saturation phenomena expected at high parton

number densities [3, 4]. In addition these upgrades will give greater coverage for the direct photon-jet measurements, critical to the measurement of the spin dependent structure functions, and photon decays of the charmonium states such as the $\chi C \rightarrow J/\psi+\gamma$ for the study of charmonium suppression in heavy ion collisions.

II.PHENIX FORWARD CALORIMETERS (NCC'S)

UPGRADE LAYOUT AND NCC CONFIGURATION

Currently the PHENIX Forward (Muon) spectrometers (Fig. 1, bottom) are limited to identifying muons and measuring their momenta via the muon tracker (MuTr) and the muon identifier (MuID). The proposed upgrade to the forward spectrometers is shown diagrammatically in Fig. 2.

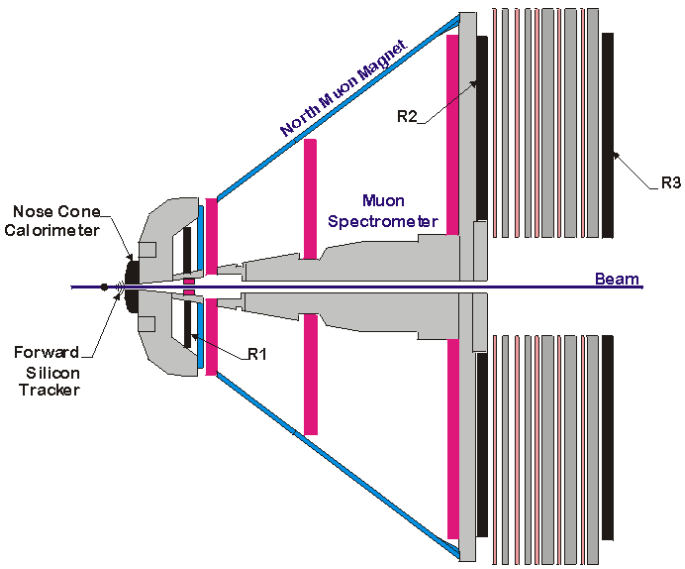

Fig. 2 Schematic rendering of the new PHENIX Forward Spectrometer. R1-R3 – resistive plate chambers built for triggering on muons.

The three principal components to the upgrade are: 1) an enhanced muon trigger that processes signals from the R1-R3 trigger chambers which is able to recognize muons and impose cutoffs on the muon pointing and muon momenta at a RHIC rate of 10 MHz 2) a forward Si vertex detector for identifying secondary vertices (FSVT) and 3) a compact W-Si sampling calorimeter (NCC) built to identify and measure forward electromagnetic activity and provide jet identification and coarse jet energy measurements. It is this third component which is the subject of this Concepual Design Report.Available real estate is shared between the Forward Silicon Tracking, the Central Silicon Vertexing System, Hadron Blind Cherenkov Detector and Nose Cone Calorimeter, the location of the latter is explicitly shown in the next picture (Fig. 3) presenting current PHENIX vision of the space allocation in the central region of upgraded PHENIX.

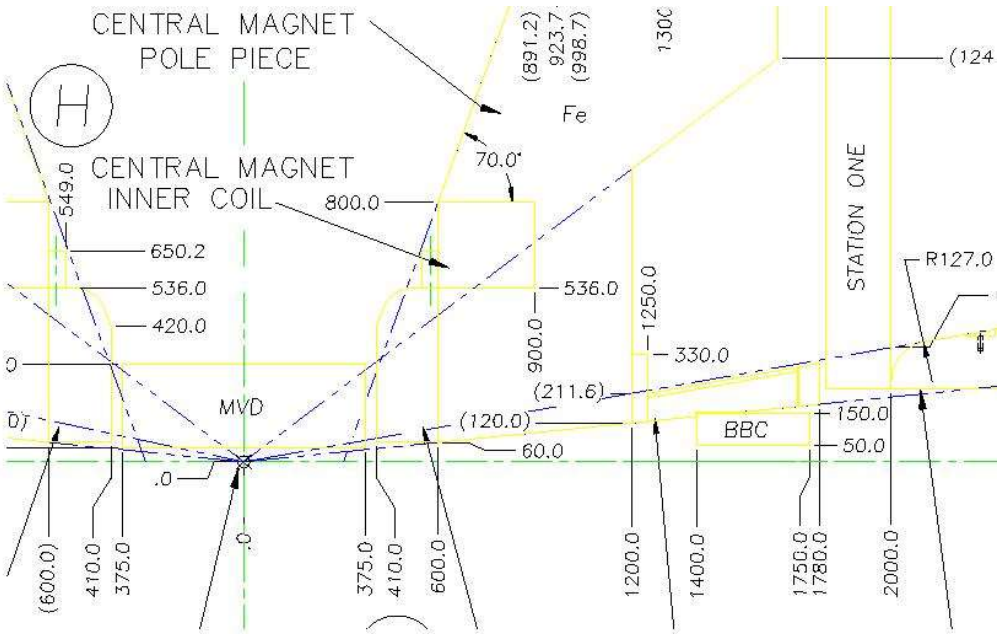

Fig. 3 Sharing of the space budget between new detectors in the central PHENIX region.

The NCC will occupy the space along the collision axis which is currently used by supplementary muon filters (NoseCones, one for each magnet pole) consisting of Cu disks 19 cm deep and ~ 1m in diameter. The depth of the new calorimeter is chosen to fit within the envelope of the existing Cu Nose Cones. We propose to build two identical devices for the North and South Arms of PHENIX. 3-d rendering of the PHENIX central region with all new silicon-based sensing devices installed is presented in Fig.4 below.

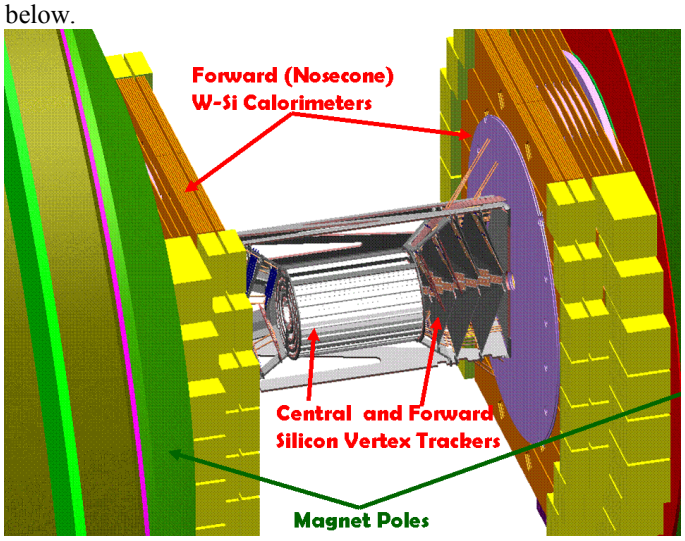

Fig. 4. 3-d rendering of the new detectors employing silicon sensors in the central PHENIX region.

As a component of the PHENIX Forward Spectrometer the NCC will provide or contribute to the following:
1) precision measurements of individual electromagnetic showers;
2) $\gamma/\pi 0$ discrimination similar to the central PHENIX electromagnetic calorimeters;
3) photon/hadron discrimination;
4) jet finding , jet energy and impact position measurements;
5) data for fast triggering.

NCC DESIGN CONSIDERATRIONS

The design considerations for the detector were defined as:
ability to measure electromagnetic showers with a precision comparable to the cumulative total of all systematic uncertainties characteristic to similar measurements with PHENIX central electromagnetic calorimeters (p0 effective mass resolution better then 20 MeV in the pT range above 5 GeV/c);

ability to discriminate between electromagnetic and hadronic showers in the calorimeter to the extent allowing extraction of the direct photon signal down to ~5% of the p0 yield;
ability to reconstruct p0's via effective mass measurements and shower shape analysis to the pT extents allowed by the calorimeter acceptance and RHIC luminosity;
ability to measure shower impact vectors with resolution sufficient for efficient matching to charged tracks reconstructed by Forward Silicon Tracking;
ability to measure the total jet energy and jet vector with precision sufficient to reconstruct kinematics of the g-q hard scattering resulting in g-jet events with jets in the forward direction;
ability to measure energies inside the jet cone around high pT lepton candidates for isolation testing.

Satisfying these specifications requires a combination of highly segmented electromagnetic and hadronic compartments supplemented by high resolution position detectors located at the depth in the calorimeter sufficient to convert both photons from ~ decay with good probability (preshower detector) and measuring decay asymmetry so the efficiency of p0 reconstruction and p0 yield are correctly measured (shower maximum detector). The NCC's are located 40 cm from the nominal collision point on both north and south poles of the PHENIX central magnet and limited to the depth of 19 cm each. Building the instrumentation capable to attain required performance under constrains of PHENIX geometry requires densest known absorber material (tungsten) and the most versatile active media known to instrumentation in physics (silicon). Silicon provides for simplicity of the transverse segmentation, tungsten has a small Molier radius (9 mm) so the showers are very compact. Tungsten also has an excellent ratio of radiation and absorption lengths (Pb has even better ratio but is much to light compared to W) what is very important for em energy measurements in the presence of heavy hadronic background.
Numerous simulations have proven that even if we rely on the utmost technology in instrumentation satisfying the whole multitude of design goals can't be achieved unless reasonable compromises are made everywhere. These compromises also require priorities assigned to different performance goals. Based upon physics expectations priorities are given to particle identification (including resolving close showers) and electromagnetic energy measurements.
A few cm of tungsten will fully absorb the electromagnetic showers; hence a properly structured 20 cm deep tungsten calorimeter can have both an electromagnetic segment and a shallow hadronic (leakage) segment. The W plate thickness and the total depth of absorber in the calorimeter are constrained by readout; it is our goal to reduce the readout space to about 2.5 mm per layer (0.5 mm silicon, 1.6 mm of pc-board, and clearance gaps).
The design of the NCC relies heavily on past experience in Si-W calorimetery [5,6,7] it is technologically challenging and nontraditional for it can't rely on momentum measurements in upstream tracking for any of particle identification purposes (in principle the integral Bdl is sufficient to identify the charge of impinging charged particle in the pT range below 20 GeV/c). Such a calorimeter covering an area ~0.7 m2 with towers comparable in size to molier radius will have ~3000 silicon pixels per readout layer. A number of ongoing R&D projects aimed to build readout for the W-Si calorimeters able to digitize signals from every pixel in every sampling layers are currently ongoing mostly within the scope of preparing the experimentation for the future electron-positron linear collider. The solutions are mostly on the drawing board and prohibitively expensive. To reduce cost and complexity we decided on a solution when geometrically matching pixels from a number of sequential silicon sampling layers are ganged together and connected to the input of a single amplification/digitization circuit.
This solution allows to reduce the number of channels in the detector by x 6 (see below), to use signal amplification solutions developed at BNL Instrumentation Department for earlier projects and to solve the problem of compatibility between new detector and existing mechanical infrastructure in efficient manner.

This document is still not a final technical detector design, some of the parameters being an educated guesses based on limited simulation studies and published documents. An essential features of our design are "as good as fiscally feasible" shower shape measurements and the spatial separation of energy depositions due to photons from those due to charged and neutral hadrons reaching the calorimeter. Very limited real estate available to calorimeter naturally suggests the same lateral granularity all through the calorimeter depth easily achievable with alternating tungsten and silicon layers.

A long and painful optimization process resulted in choosing the calorimeters built of 18 pad-structured sampling layers and two layers of 2-d position sensitive pixilated strips (preshower and shower max) which will serve as a very efficient photon-p0 identifier discriminating between individual electromagnetic showers and overlapping photons from high momenta p0's. The particle identification capabilities are due to longitudinal shower shape measurements in three sequential longitudinal segments (the first two are fine sampling and the last serving as a coarse leakage segment) and independent lateral shower shape measurements in three longitudinal segments and two high resolution position sensitive layers.

We have chose 3 mm W plates for the fist two fine sections based upon the following simple considerations.
In general the radial shower profile which is the main source of data to discriminate single vs multiple showers has a pronounced central core surrounded by halo. The central core effectively disappears beyond shower maximum. The radial profile integrated over the whole shower depth in different materials is shown in the Fig. 5.

Fig. 5 Radial profile of the electromagnetic showers in different materials

The data for Al, Cu and Pb are from [Wigmans], data for W are our simulation. The distance from shower axis is in Molier units (9.3 mm for W). W is certainly the material of choice if discrimination against multiple showers is one of the primary goals (suppressed halo). A 50% of the shower energy is contained within the radius of 0.25 Lmolier which is a back-of-the-envelope estimate for intrinsic limit for the efficient two-shower separation (further improvements are hampered by fluctuations in the number of particles in the shower). The symmetrically decaying 30 GeV/c p0 will have two photons in calorimeter at a distance of the order of 5 mm (depending on the production kinematics) thus setting the upper limit to Molier radius for NCC equal to 20 mm. Technology sets a lower limit to the thickness of readout layers (carrier boards, silicon sensors, interconnects, protection) close to 2.5 mm. To keep Molier radius below 20 mm the thickness of W plates in the fine sections of calorimeter must be equal or above the same 2.5 mm value.
As it is always with energy measurements in multy-GeV range the energy resolution is driven by the sampling fluctuations, the latter (see [Wigmans]) can be reasonably well described with the following simple formula:

$$\frac{\sigma}{\sqrt{E}} = c\sqrt{d / f_{sampl}},$$

where the thickness d of the active layers is in [mm] and fsampl is the sampling fraction for MIP's. The collection of the data presented in the Fig. 6 extacted from the same reference agree well to this parametrisation (within 10%) with coefficient c ≈ 2.7%.

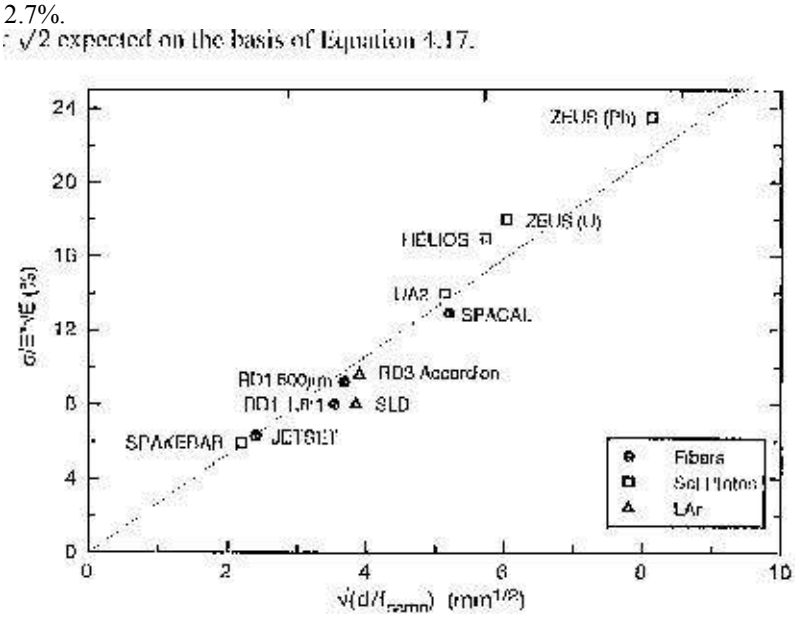

Fig. 7 Compilation of data on energy resolution of the sampling electromagnetic calorimeters [Wigmans].

The calorimeter built of 2.5 mm W plates and 2.5 mm readout layers (525 mm Si sensors) will sample approximately 2.9% of energy left in the calorimeter by minimum ionizing particles resulting in the energy resolution close to

$$\frac{\sigma}{E}; \frac{25\%}{\sqrt{E}}.$$

The NCC is supposed to discriminate electromagnetic and hadronic showers based upon shower shape measurements only. To make this approach effective it must retain its declared energy resolution towards the limit set by physics (requires reasonable longitudinal containment within fine sections for electromagnetic showers) and a total shower energy measurement (including hadronic showers) well downstream of the total depth required to contain electromagnetic showers. We propose to build electromagnetic segments of 3mm W/2.5 mm readout sampling cells. 12 sampling cells combined with 2 Lrad upstream converter comprise close to 12 Lrad electromagnetic calorimeter with energy resolution ~27%/$\sqrt{E}$ sufficiently deep to contain at least 90% of the electromagnetic shower energy. Two layers of precision position sensitive silicon detectors will be located downstream of converter and between two fine sections (at approximately a shower max depth) to discriminate single vs multiple photons and to measure decay asymmetry. A single calorimeter tower thus structured is sketched in Fig.8.

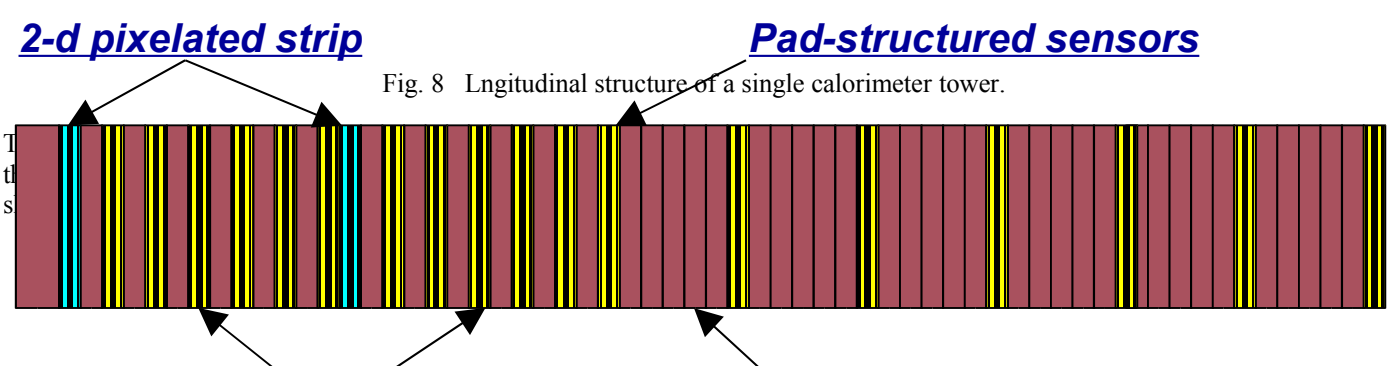

Fig. 8 Lngitudinal structure of a single calorimeter tower.

sampling cells of a lateral size identical to that in em sections. It will (1) assist the energy measurements of photons at the extreme upper end of the spectrum); (2) serve as an effective em/hadronic discriminator tool; and (3) assist with low grade jet energy measurements .t Leakage section will use all remaining available longitudinal space within 19 cm real estate currently reserved for calorimeters. Subtructing the space needed for 2 Lrad converter, two 5 mm thick layers of position sensitive detectors and twelve 5.5 mm sampling cells which comprise electromagnetic calorimeter the space left for leakage compartment is equal to 10.7 cm. (6 cells of 15 mm W and 2.5 mm Si readout layers).

The total depth of calorimeter seen by particles at normal incidence is ~42 Lrad or 1.6 absorption length. Short summary of the calorimeter design featues is in the Table 1 (all counts are for a single calorimeter unit).

Parameter		Value	Comment
Distance from collision vertex		40 cm	
Radial coverage		50 cm	
Geometrical depth		~19 cm	
Absorber		W	42 Lrad or 1.6 Labs
Readout		Si pads (15x15 mm2) and pixeleted strips (.0.5x0.5 mm pixels grouped into 60 mm long strips)	
Calorimeter		EMC(12 sampling cells: 3mm W + 2.5 mm readout) longitudinally structured into two identical nonprojective sections. Leakage(6 sampling cells: 15 mm W + 2.5 mm readout)	
Preshower detector (PS)		2 Lrad W converter followed by a stripixel layer (0.5 mm strips) with 2-d readout	
Shower max detector (SM)		In between two EM sections at ~ 7 Lrad depth. Stripixel layer (0.5 mm strips) with 2-d readout	
Sensors		calorimeter	3192 (12 x 168 + 6 x 196)
		PS and SM detectors	336 (2 x 168)
Channel count		calorimeter	8152
		PS and SM detectors	86016 (672 SVX4 chips)
Multiple scattering in NCC combined with Fe magnet pole		133 MeV	To compare with 106 MeV in the existing configuration with Cu NoseCone
Expected EM energy resolution		$27\%/\sqrt{E}$	
Expected jet energy resolution		$100\%/\sqrt{E}$	
Two showers resolved at	in calorimeter	3 cm	
	in preshower	2 mm	
	in shower max.	4 mm	

Table 1. Nose Cone Calorimeter design featues

NCC DYNAMIC RANGE CONSIDERATIONS

In NCC the energies of the showering particles will be shared between thee segments of the calorimeter. In principle this sharing is uneven, most of the electromagnetic energy will be deposited in the second, most of hadronic energy in the third or leakage section. Accounting for fluctuations and lateral energy sharing it is sufficient to set the upper limit of dynamic range per tower per section close to ~ 60% of the W mass to cover the whole range of physics topics we are planning to study in pp-interactions at a 1 TeV collision energy.

Since the NCC is close to the production vertex, the calorimeter will need to work in at high occupancy, especially in central Au-Au collisions. The calculations were made assuming that any shower in the calorimeter would always fire a base matrix of 3x3 towers and 3 neighboring strips in the SMD. The strips and towers were assumed to be of a similar surface area (~200 mm2) what is grossly exaggerated for the SMD version as per this proposal. The resulting radial (from the beam) dependence of the probability for strips in the SMD and towers in the calorimeter to see event related energy is plotted in Figure 9 below.

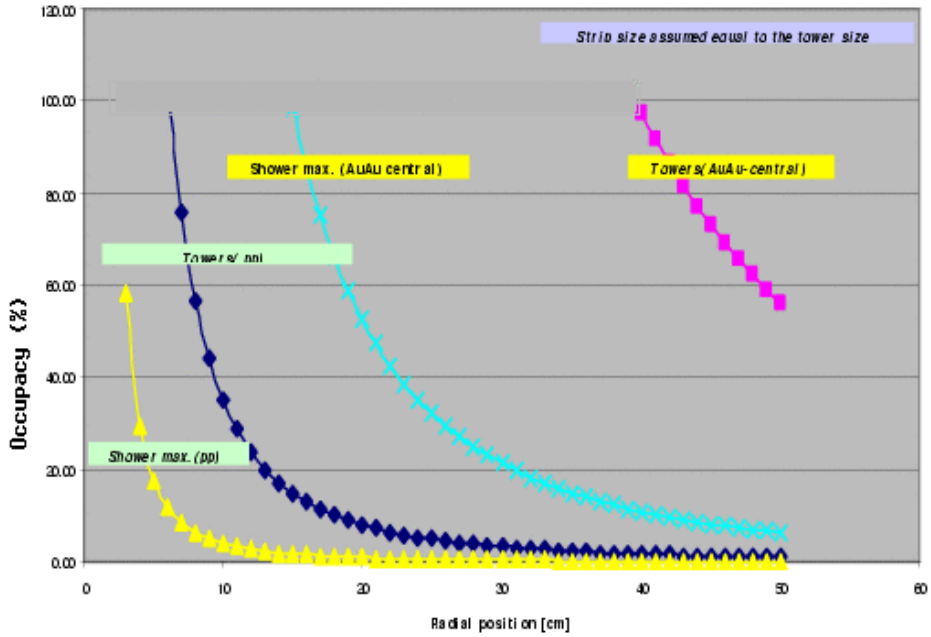

Fig. 9 Probability for Tower in NCC and strip in SMD to be fired (occupancy) in pp and AuAu collisions in PHENIX as function of the distance from the beam pipe.

In pp collisions, conditions similar to those in the central calorimeter are reached at a radial distance of 10 cm hence the entire calorimeter area will have a reasonable occupancy. The beam pipe assumed to be 4 cm in diameter. Running conditions are certainly less favorable in AuAu collisions where the calorimeter will be heavily occupied by the showers due to soft secondary particles. The SMD occupancy still stays relatively low for cluster counting and impact point measurements in the calorimeter allowing jet finding based upon hit occupancy even in the events of highest multiplicity. Energy measurements in AuAu collisions will be strongly affected by the pileup from underlying events resulting in higher threshold values and additional inefficiencies. Simillar problems are seen in the present central caloimeters. Jet measurements are certainly the most challenging part of NCC program. Multiple approaches such as threshold selected hit counting, energy profiling and energy flow should be tried. The next figure (Fig. 10) is a crude example of what to expect in pp collisions.

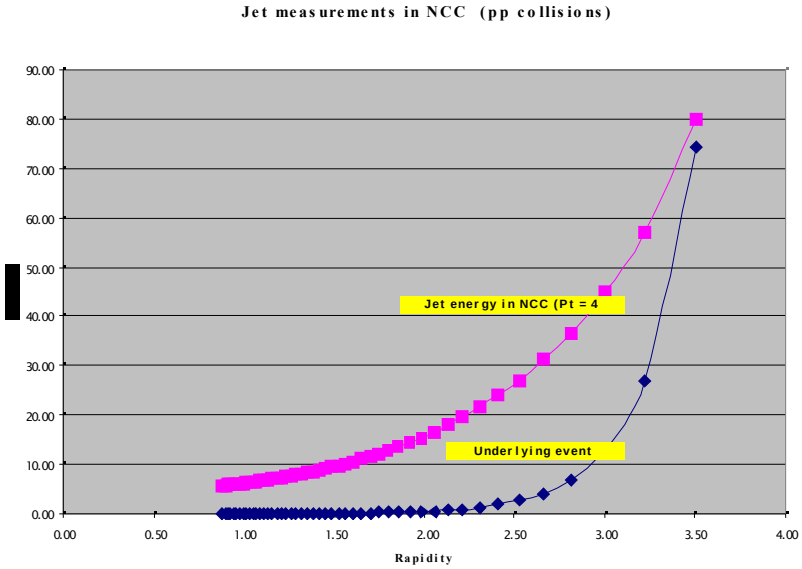

Fig. 10 Effect of the underlying event on the jet measurements in the Nose Cone Calorimeter in pp collisions at RHIC.

Depending on the rapidity, a 4 GeV/c transverse momentum jet in the NCC acceptance window will have a total energy of 8 GeV to 80 GeV. It will be seen in the calorimeter with very little pileup contribution up to ~2.5 units of rapidity and will start merging with the underlying event only at rapidity ~3. In pp collisions a dense relatively shallow calorimeter will see high pt jets as easily identifiable, narrow peaks in the energy profile. Due to the background from underlying events in Au-Au collisions, there will be more smearing to the energy profile which will move the threshold for identifiable jets to somewhat higher transverse momenta.

NCC MECHANICAL DESIGN

A modular NCC design emerged as an outcome of a study of a different approaches to mechanically structuring future detector is illustrated in Fig. 11.

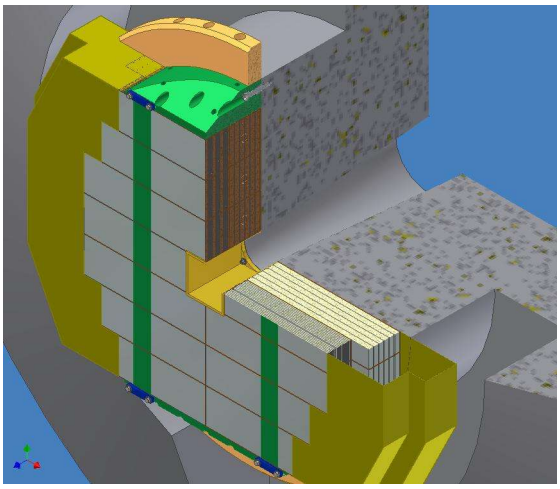

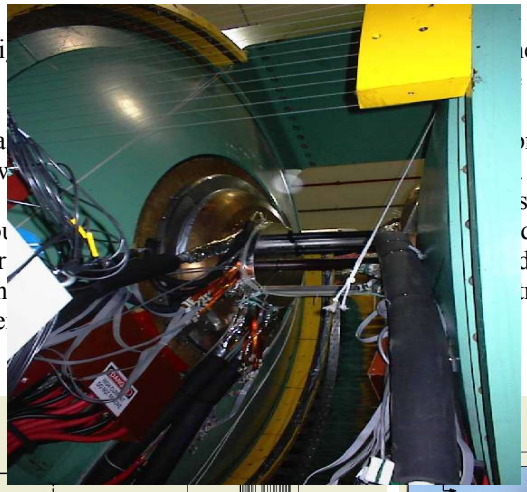

Fi ne Calorimeter (right panel). Boxes upstream are with electromagnetic segment. Air plenums housing preamplifiers are also shown.

The ca bricks (see Fig. 12) used to build two quasi-independent calorimeters: shallov . All bricks are single sensor wide, there are three standards for the brick length sensors in hadronic, 6/5/4 sensors in electromagnetic sections). Readou demanding compared to hadronic. Electromagnetic brick will house conver d two electromagnetic segments, hadronic brick will consist of a single hadron tream and Cu skin locking it on all other sides except one for connections to exte

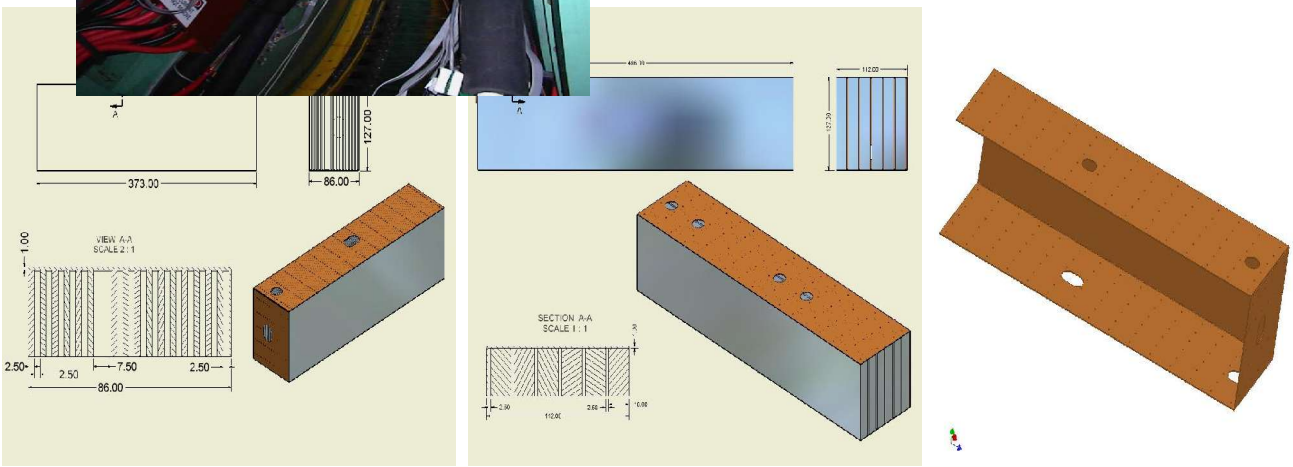

Fig. 12 NCC building bricks. Left – electromagnetic. Wide gaps indicate locations for preshower and shower max detectors. Center – hadronic (leakage). Cu skin for the electromagnetic brick is shown on the right.

When assembled bricks will form two vertical walls, small locking pins will be used to maintain the geometry. For mechanical reasons the two walls will have the same size vertically (giving up some of the hadronic acceptance), horizontally hadronic wall is two sensors wider compared to electromagnetic wall. This geometry allows to minimize the cost while keeping all light rays from the nominal collision point to the currently existing brass cones within calorimeter structure. Calorimeter walls are supported by two (bottom and top) shelfs and thin pretensioned front braces (strips of stainless steel or kevlar) preventing walls from buckling out.

NCC SILICON DETECTORS

The main requirements for the silicon detectors in the calorimeter are reliability, precise shower energy measurements via charge measurements in silicon, precise tracking measurements, and radiation hardness. The solution to the problem is arranged using multilayered device built of pad-structured layers organized into towers in readout and strip-structured layers (pixelated strips in our case) to track individual charged particles and resolve close showers. The pad size chosen for NCC is 1.5x1.5 cm2, the strip size is 0.5x60 mm2, all silicon detectors in NCC are 6x6 cm2 diced of 4" wafers 525 mm (pad structured) and 600 mm (stripixels) thick. Critical to the success of the experiment will be reliable operation of these sensors in a radiation environment. The estimates based upon total energy flow simulation predict the total fluence of 100 kRad (in Si) or about 3*1012 equivalent neutrons per cm2 over the period of 10 years (assuming pp interactions at 200 GeV with luminosity ~2 1032 s-1cm-2). For a pad size of the order of a few cm2 and 300 mkm sensor thickness, published data predict the leakage current of the order of 5 – 10 mkA per pad. Handling this value of current definitely requires decoupling capacitances being present between pads and preamplifiers,

For the operation of the detectors the control of leakage current is important not only because it leads o increased noise. It may also result in the increased bulk heat production in silicon which may lead to thermal runaway if the silicon detector is not cooled. In our design of sensors and selection of raw material we were guided by the experience and work done within the scope of D0 (FNAL) and ALICE (LHC) projects and recent published data from the research and development in the radiation hard silicon technology. In particular we followed few simple and well known rules:

single sided sensors from established vendors to insure higher yields and less trouble due to simplicity of the design. It is also well known that double sided sensors are the once suffering radiation damage;

minimal number of different sensor designs (only two in NCC case);

design to successful completion of he project using single vendor. Transfer the design to additional vendors when ready. This will speed production;

use short strips to reduce the number of ghosts hits otherwise creating pattern recognition hassle (we use 4" wafers only);

avoid double metallization. Reasons are not 100% clear, but we followed this recommendation too;

special designed guard ring structures. Such guard rings are important in order to keep breakdown voltage before and after irradiation as high as possible.

In short for the construction of the Nose Cone Calorimeters we will use the single–sided single-metal p+ on n-bulk silicon devices. We also to have an integrated polysilicon resistors on the sensors to simplify the test procedures (sensor can be fully depleted using two lines only) and to minimize the real estate used by external RC chains to DC couple detectors to readout electronics (crucial in the strip sensors). Two kinds of sensors are used to construct NCC's : pad structured and pixilated strips. They both will be described in more details below. The pad-structured sensors has many prototypes, this technology is well tested and we already have three established vendors ready to manufacture the 6x6 cm2 pad-structured sensors using common design files (corrected for specifics of technology). The pixilated strips (stripixels) are novel detectors developed at BNL and currently selected as a base design for silicon sensor for the PHENIX central silicon tracker. The design chosen by PHENIX are interleaved stripixel detector where each pixel is divided into two parts: X-cell (or pixel) and Y-cell. X-strips and Y-strips connect X-cells and Y-cells, respectively, in a strip detector readout scheme. In this detector two dimensional (2D) position sensitivity is achieved with single-sided processing. Short summary of sensor parameters is given in Table 1.

Specifications	Pad-structured sensors	Stripixel sensors
Wafer thickness	525 mm	600 mm
Depletion voltage	100-120 V	130 – 155 V
Diod capacitance	37 - 41 pF	
Bias voltage	Full dep. V + 20V	Full dep. V + 20V
Leakage current	<300nA total, <20nA/pad	<1A total
Junktion breakdown	> 300V	> 300V
Implant area	15 x 15 mm2	TBD
Al area	15.02 x 15.02 mm2	15-60 mm prototyped. Decision pending.
Polysilicon bias resistor	1 m	1 m
Interpad (strip) capacitance	< 2pF (pad-pad) or < 8 pF (pad-all neighbors)	TBD
Maximum heat dissipation from the bulk material	< 50 W	< 100 W
Heat dissipation from on-the-sensor electronics	-	TBD

Both sensors have been prototyped at ELMA (Russia) and are currently investigated.

Pad-structured sensors and pad-structured readout layers

The calorimetric energy measurements are based upon ionization charge left by shower particles in the layers of pad structured silicon sensors. We are also considering using signals from preshower detector to compensate for the energy loss in the first 2 Lrad of W used to convert photons. The pad structured Si layers (18 in total) interleaved with W plates 3 mm (in

electromagnetic) and 15 mm (in hadronic) segments are built of 6x6 cm2 silicon detectors subdivided into 16 identical square cross section pads (diods).
Test pad-structured DC coupled silicon sensors optimized for radiation hardness following the prescriptions above were recently produced at ELMA foundry in Moscow suburb and delivered to our collaborators laboratory at MSU. The actual sensor picture together with the guard-ring structure are shown in Fig. 13.

Fig. is subdivided into 16 readout pads 1.5x1.5 cm2 each. On the righ gn is to prevent voltage breakdowns after radiation exposure.

5k, e at MSU were used for this submission. In total 30 sensors wer sensors accepted and 5 sensors rejected (large leakage currents). Res easurements are shown in Fig. 14.

Fig. Rus

We a pr was para and

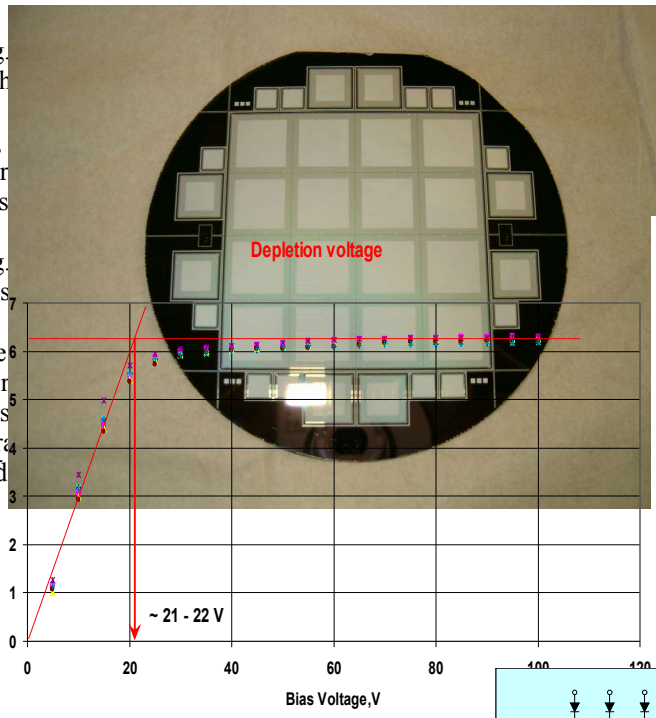

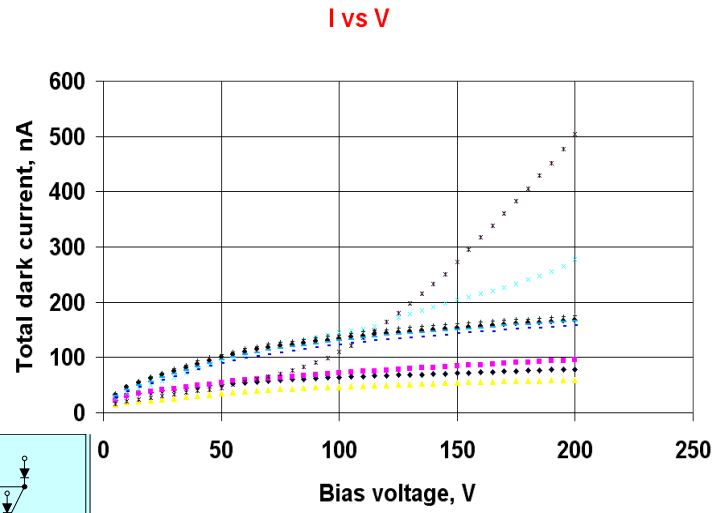

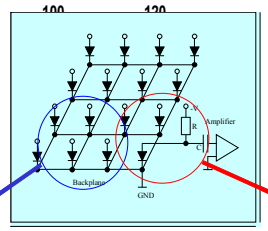

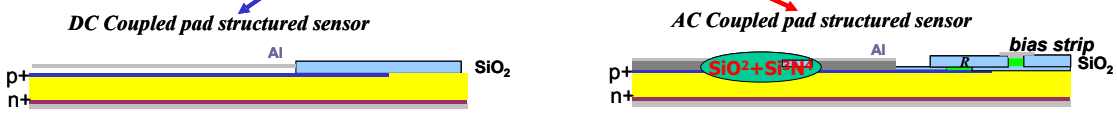

Fig. 15 Two extreme desines for the pad-structured Si sensors. DC on the left and AC on the right.

The sensors with built-in RC networks are probably the only option for detectors planning to digitize signals from individual pixels. Unfortunately this technology routinely results in increased cost and reduced yield associated with extra steps required to grow large capacitances on pad surfaces. In case of PHENIX NCC where individual pixels are ganged together to allow a single preamplifier to handle analog sum of the pixel currents the advantages of AC coupled design are not obvious at al, it may result in ineffective spending of resources. Our project was recently reviewed by the unofficial panel of Si detector experts at SiDet Laboratory at FNAL, the recommendation which we accepted was to retain the polysilicon resistors on the sensors and to use external decoupling capacitances. Modified design is now available to ELMA (Russia), ON Semiconductors (Czech Republic) and SENS (Korea) foundries, we expect new sensors for evaluation and system prototype construction delivered first trimester of the next year.
The sensors will be mounted on the sensor carrier pc boards, Sensors, carrier boards and interconnects (see Fig. 16) form readout unit the latter installed in the gap between W plates, its positioning is defined by the locking pins on the side opposite to sensors.

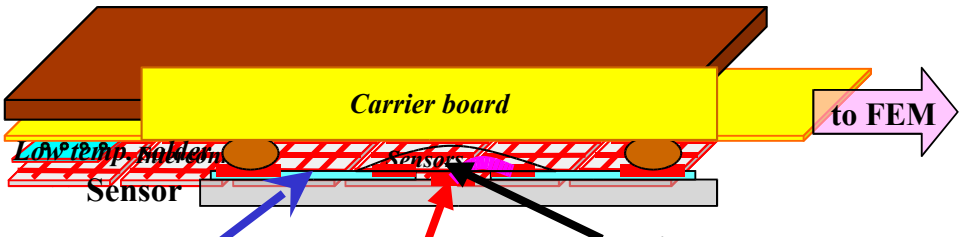

Fig. 16 NCC Readout unit structure. Details of the sensor installation scheme are in the bottom part of the picture.

The interplate gap reserved for readout unit is 2.5 mm thick. 0.5 mm of this space is silicon, ~1.2 mm is FR4 (motherboard), 0.2 mm is the FR4 interconnect, another 0.2 mm is the FR4 spacer required to control the height of low temperature solder between interconnect board and carrier board. Remaining ~0.4 mm gap is to insure that no pressure is applied to the surface of Si sensors what otherwise may result in increased noise due to piezoelectric effect.
This particular design which may still undergo further modifications is chosen because of a promice of repearbility for assembled readout unit. Soldering points are connected to the bonding pads via traces what allows to locate them around center of the interconnect board. If sensor fails it will take heating just the central area of the sensor to remove the sensor with interconnect board from the carrier board. New sensor assembly will then be installed (soldering points will require cleaning and new dose of paste).
The NCC will use four different standards for the readout units: all single sensor wide with the number of sensors varying between 3 and 7.

Stripixel sensors and stripixel readout layers
One of the major tasks NCC will need to complete is to study direct photon production in events with correlated photon-jet in the final state resulting from compton scattering of soft gluon on a quark. This is probably he most revered process as concerns our ability to access the partonic evolution in the initial state leading to sQGP formation. The background to this process are the double-jet final states with one jet fragmenting into leading p0 faking single photon due to shower overlaps. In the detector built of composite material with Molier radius rM ~18 mm and characteristic slope of the shower core ~0.2 rM = 4 mm, the clear separation of the maxima due to two photons with close energies is possible down to a similar value of ~0.2 rM.
The problem arises when attempting to prove that observed maxima do really due to independent showers and not to the shower fluctuations. The separation is too small compared to the average shower radius at the same energy to make meaningful qualitative testing based even on the most detailed lateral shower shape measurements. The following strategy is adopted for NCC deal with fluctuations. We are installing two layers of identical 2-d position sensitive detectors (0.5 mm pitch) in the calorimeter at two depths: 2 Lrad and 7 Lrad. The first layer (preshower) installed downstream of 2 Lrad W converter is a hit counting layer where position resolution is limited by the strip width to ~150 mm, the second (shower max) layer will serve to measure decay asymmetry (if two showers are expected) through the shower shape analysis at a depth where the shower expands to rM radius. Simulation have shown that this approach will work well to 0 energies above 30 GeV (effectively to the limit set by integrated luminosity we can hope for). We have chosen a novel detector of interleaved pixilated strips ("stripixel") developed at BNL and already in use for the Central Silicon Tracker in PHENIX. This novel detector generates X-Y two dimensional position sensitivity with single-sided processing and readout . Fig. 17 is an illustration of the concept. Comb shaped structure with 250 m prongs cover the pixel area 500x500 mm2. Prongs are interleaved with similar prongs from two overlapping pixels on the right and on the left.

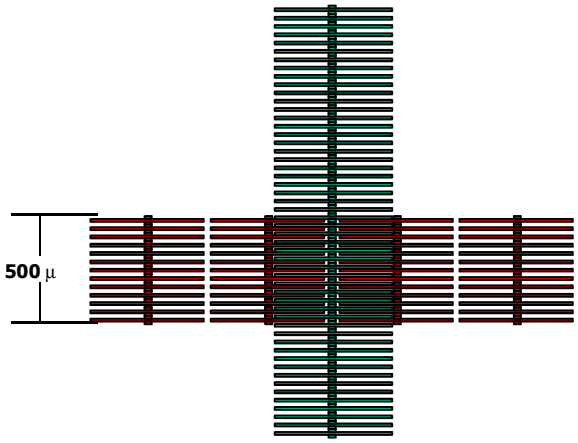

Fig. 17 Design of the detector with interleaved pixilated strips with 2-d position sensitivity. Ionization charge produced by charged particles in Si is shared between X and Y oriented strips.
Alternate combs are connected either in X direction (forming strip measuring Y coordinate) or in Y direction (for X measurement).Pitch between prongs belonging to different strips is chosen comparable to charge diffusion to insure uniform charge sharing. While it is easy to predict that an optimal pitch for 525 m wafer must be in the range of 15 mm, it may still be affected by the comb geometry and needs prototyping and infrared laser or beam testing before the project commits itself to one particular value. Another critical issue are interpixel connections and crosstalks, the latter depend on the total length of the strip edge which in turn is correlated to the pitch. While PHENIX Central Tracker employs the double metal technology for interpixel interconnects, it may be of advantage to the Forward Calorimeters to use a different technology with better promise for radiation hardness. The n+ implants create conductive regions in the bulk silicon separated from Al with a layer of SiO2.
To test different versions of the comb structure BNL Instrumentation (Zheng Li) produced the design for the 6x6 cm2 test stripixel sensor with bands of X and Y strips 20-strips wide (short strips crossing the bands are all connected together to simplify crosstalk measurements). Sensor has 5 stripixel configurations prototyped, all strips are connected to bonding pads via local pitch adaptor (Fig. 18).

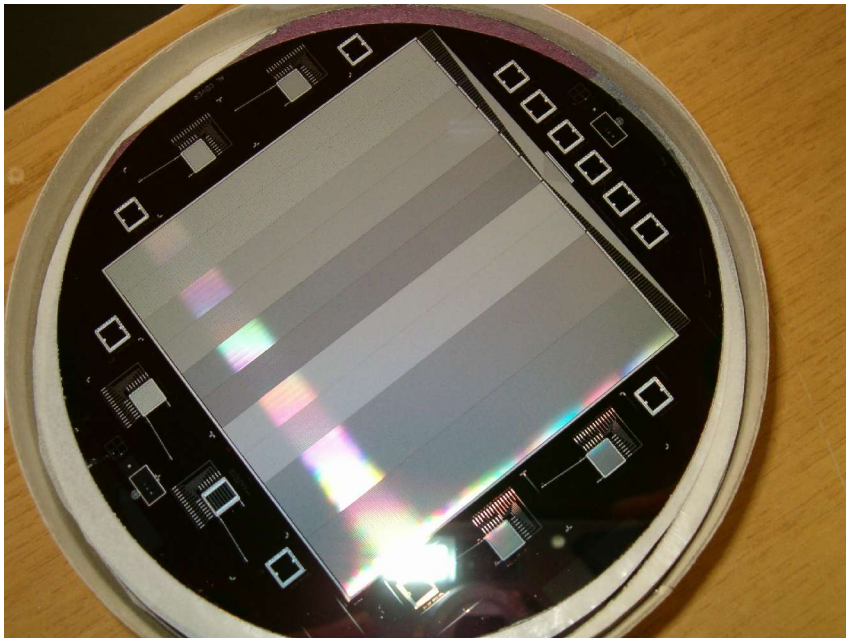

Fig. 18 Si wafer with stripixel test structure designed in BNL Instrumentation Department and produced by ELMA in Russia.

Measurements of depletion voltages using on-sensor test structures have shown that wafer processing was done satisfactorily (Fig. 19). Test sensors are expected to be fully functional and fit for further testing.

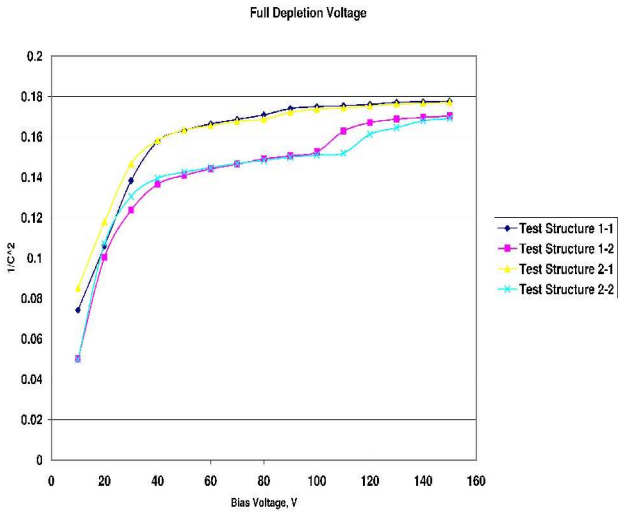

Fig. 19 Preliminary results of depletion voltage measurements on a test structures on the new stripixel sensor for the PHENIX NCC.

The readout system for the stripixel silicon detectors will be based on the SVX4 chipo and the existing PHENIX data acquisition system. Strips are connected to DCM's through hybrids with RC network and SVX4 chips daisy chained and followed by interface board with sequencer which are in turn connected to DCM's. The hybrids will be glued directly onto the sensors with a common of the sensor glued to carri board. A very preliminary design of the hybrid is shown in Fig. 20 with a carrier board and sensor.

Fig. 20 Design of the interconnect (hybrid) with external RC network and SVX4's for the NCC stripixel layer.

NCC ANALOG SIGNAL PROCESSING

For readout purposes the calorimeter is longitudinally segmented into two fine and one coarse sections (two electromagnetic and one shallow hadronic compartments) and two 2-D sensitive coordinate section. In total the silicon tungsten calorimeter as it was described above will have close to 60 000 silicon pixels and 80 000 strips. This calls for a compact, economical readout. Depending on the location in the calorimeter the readout unit will deliver between 48 and 112 signal lines to the preamplifier board. Following the declared intent to minimize the number of individually designed components in the detector, we are planning to use the same design of the adapter board everywhere with only live channels populated.
We will sum up all depth-sequenced pixels in each longitudinal segments of the calorimeter. A simple passive (on the resistors) summation scheme will be implemented on the outskirts of the detector (signals from individual pixels are sent to the summer via traces on carrier board). Rather modest goals for the electromagnetic energy resolution as set in this proposal allow us to disregard the potential contribution to resolution due to the spread in the gains between individual channels. Summed signals are amplified using hybrid tranceresistance amplifiers developed at BNL for ATLAS liquid argon calorimeter. Modifications to the existing design will include polarity change for all transistors (to work for positive swing signals) and adding differential drivers to drive the signals over twisted pairs cables to the digital signal processing plant. Block diagram of the analog signal processing plant is shown in Fig. 21.

Fig. 21 NCC analog signal processing block-diagram

NCC DIGITAL SIGNAL PROCESSING

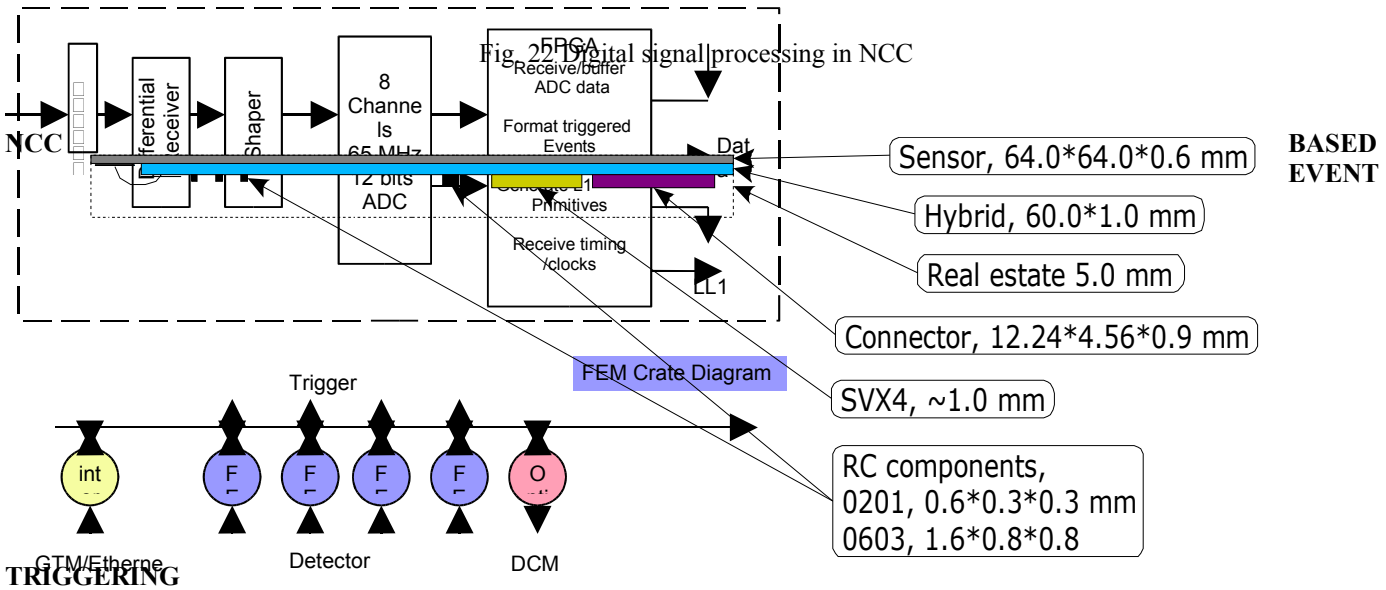

Fig. 22 Digital signal processing in NCC

TRIGGERING

In order to pursue it's rare-event physics program the PHENIX experiment requires high luminosity from the RHIC accelerator and highly selective Level-1 and Level-2 trigger systems. In particular, the Level-1 trigger system is limited to a maximum rate of 12.5kHz by the readout rate of the detector front-end electronics. This will require an overall event rejection of up to ~1000 when RHIC reaches its goal of ten times design luminosity for protons in future runs. Since we anticipate the parallel acquisition of several rare event channels, the rejection for an individual trigger channel must be larger by a factor 5-10. The PHENIX Level-1 trigger is fully pipelined and provides an event decision in less than 4.2μs (40 RHIC clock ticks).

The PHENIX Level-1 Trigger is a parallel, pipelined trigger system designed to provide a highly configurable trigger capable of meeting the demands of the PHENIX physics program. The Level-1 Trigger consists of two separate subsystems. The Local Level-1 (LL1) systems communicate directly with the participating detector systems. The input data from these detector systems is processed by the LL1 algorithms to produce a set of reduced-bit input primitive data for each RHIC beam crossing. The Global Level-1 system receives and combines this data to provide a trigger decision. In addition, busy signals (both global and trigger) are managed by GL1. The PHENIX detector system readout is divided into two sets of elements: granules and partitions. A granule is the smallest detector element that communicates with the PHENIX timing and control system via a Granule Timing Module (GTM). The GTMs distribute the local 9.4Mhz RHIC beam clock as well as control bits and event accepts to the granule. A partition is an administrative configuration of granules that share both busy signals and Level-1 triggers.

In this PHENIX upgrade the nosecone calorimeter (NCC) LL1 primitive system will generate primitive information on the jet axis, as well as single and multiple high energy clusters. A possible muon tracker LL1 system will generate primitive information on the momentum of high pT tracks.
The MuID LL1 system is based on a generic, configurable LL1 trigger board designed and built by Iowa State University. The Generic Local Level-1 hardware (GenLL1) was designed to address a number of difficulties faced in extending the original design concepts for LL1 systems to address the full range of PHENIX trigger needs. First, the hardware had to be re-programmable to allow not only quick corrections to the trigger logic, but modifications of the trigger system as the PHENIX physics program evolved. This also had the added advantage of lowering development costs and allowing quicker prototyping of new trigger systems. Second, the new hardware had to be able to manage a data throughput of ~20Gb/s in order to be able to handle large data volume detectors (such as the Muon Identifier) without prohibitive cross-stitching between multiple boards (and crates of boards). Finally, in order to keep power consumption and heat load on the board within reasonable limits the GenLL1 design was required to use the next generation of HP GLINK receiver/transmitter logic (the HDMP 1032/1034), which runs at 3.3V. Smaller format transceivers (Agilent HFBR 5912) were also required in order to be able to handle up to twenty fiber inputs on a single 9U VME board. A complete description of the GenLL1 hardware can be found elsewhere.

In order to maximize the trigger rejection at Level-1 it will be necessary to combine trigger information from all of the forward Level-1 systems. In order to accomplish this, a new regional trigger processor will then take the complex trigger primitive information from the nosecone calorimeters, muon tracker systems and muon identifiers, combine the individual detector LL1 primitives, make trigger decisions and send them to GL-1. A block diagram of the data flow is shown in Figure 1. In order to pass data between the regional trigger processor and the LL1 systems efficiently it may be possible locate all the Level-1 trigger systems in a single crate and make use of a high-speed 16-bit data bus that is already available in the GenLL1 design to transfer the trigger primitives.

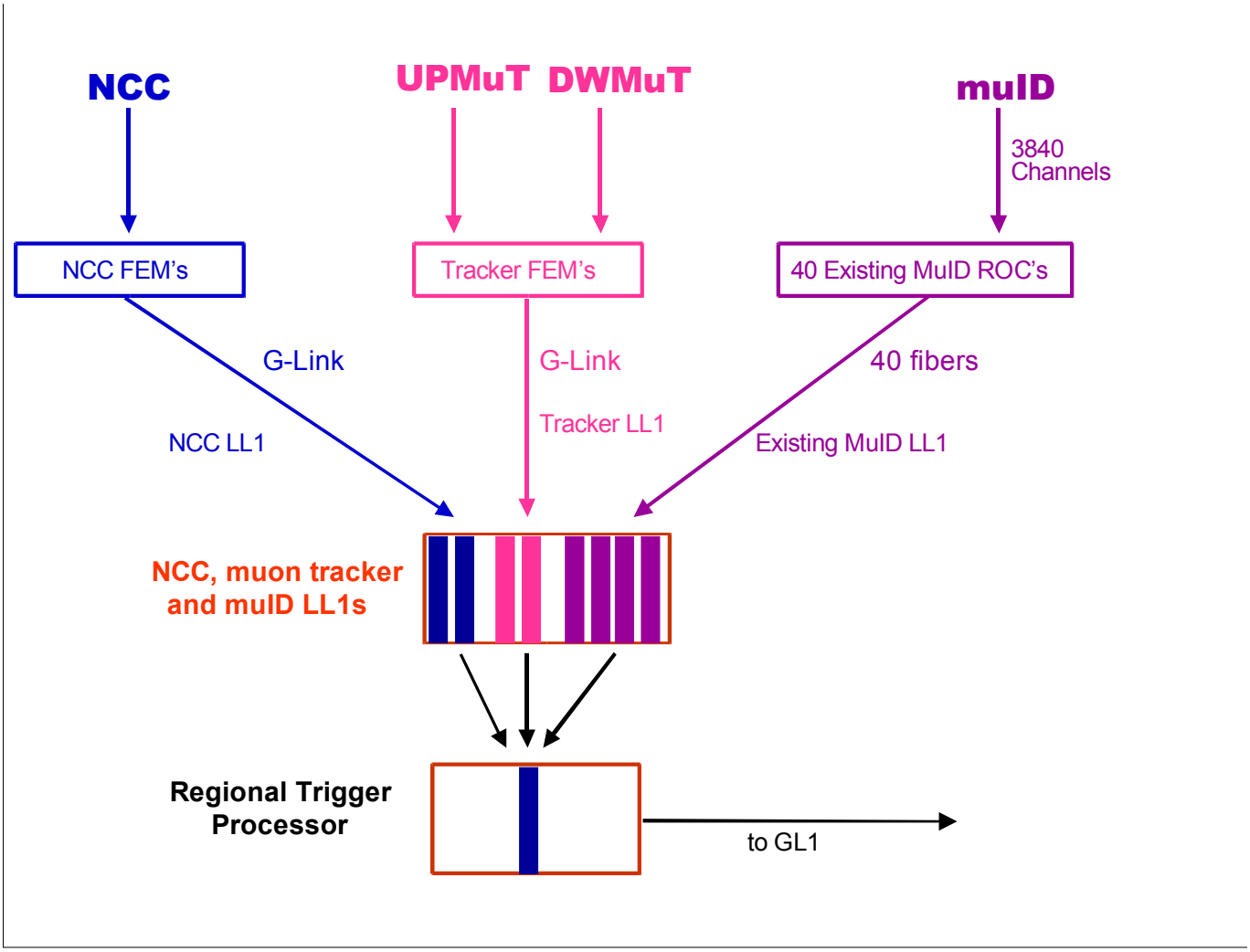

Fig. 1. Block diagram of the combined forward PHENIX Level-1 trigger system showing the nosecone calorimeter, NCC, trigger muon tracker stations and the existing MuID LL1 system for a single PHENIX muon arm. In order to combine the primitives of the various trigger systems a regional trigger processor will combine the trigger information before sending primitives to Global Level-1.

The NCC Level-1 Trigger System

The nosecone calorimeter (NCC) will use a Local Level-1 (LL1) trigger to select events via with a high pT photon or jet in the calorimeter acceptance. As is typical of PHENIX LL1 systems the processing will consist of a set of pipelined stages. First, a set of primitive data will be digitized on the front-end modules (FEMs). Second, this data will be transferred to an LL1 system, and finally the bit-reduced trigger information is sent from the LL1 system to the PHENIX Global Level-1 trigger system; possibly via a new regional trigger processor to combine level 1 information from the different forward detector systems.

The NCC system consists of over 10k channels of analog data per nosecone spread over three layers in depth. The FEMs will combine calorimeter towers into non-overlapping 2x2 trigger tiles, digitize the output, and pass the LL1 system an 8-bit ADC value per trigger tile. The 8 bits per channel will allow a ~400 MeV least count with a full range of 100 GeV, and will result in an aggregate bandwidth of 200Gbit/s per nosecone into the LL1 system, roughly a factor of 5x larger than the data processing capacity of the existing MuID LL1 system.

Because of the large data volume and tight space constraints on the detector FEMs we are considering the possibility of transferring the data over high-speed serial links into an LL1 system located in the detector hall, as opposed to other LL1 systems that transmit their data over optical fiber links to LL1 electronics in the PHENIX rack room. The advantage of this approach would be that with serial links we could concentrate the entire NCC LL1 data stream into a smaller number of LL1 modules, simplifying the data cross-stitching required for jet cluster trigger algorithms. This would only be possible by using high-speed

copper serial links between the detector FEMs and the LL1 electronics which are inherently short-range, requiring the LL1 electronics to be located in the detector hall.

The LL1 system would process the NCC 2x2 data to provide a set of photon triggers and jet cluster triggers based on the 2x2 trigger tiles, where both sets of algorithms would operate both laterally and using the depth information in the NCC to provide clean photon triggers. Detailed simulations of the performance of the NCC LL1 system are underway. The reduced bit output of the NCC LL1 trigger, in the form of a set of bits indicating satisfied algorithms, would be transmitted to the GL1 system over optical fiber.

The NCC will participate in a local-level-1 trigger (LL1) to select events with a high pT photon or jet in the calorimeter acceptance. The processing will consist of a set of pipelined stages. First, primitive data will be built of bit-reduced digitized measurements. Second, this data will be transferred to a LL1 system, and finally, further bit-reduced trigger information will be sent to the global-level-1 trigger (GL1), via a new regional trigger processor combining level-1 information from the different forward detector systems.

The single NCC system consists of about 8k channels of analog data per nosecone, spread over three layers in depth. The local processing units will combine calorimeter towers into non-overlapping 2x2 trigger tiles and pass the LL1 system an 8-bit ADC value per trigger tile. The 8 bits per channel will allow a ~400 MeV least count with a full range of 100 GeV, and will result in an aggregate bandwidth of 200 Gbit/s per nosecone into the LL1 system; this is roughly a factor of 5 times larger than the data processing capacity of the existing PHENIX LL1 system.

We are considering the transfer of data over high-speed serial links into an LL1 system located in the detector hall as opposed to other LL1 systems that transmit their data over optical fiber links to LL1 electronics in the PHENIX rack room. The advantage of this approach would be that with serial links we could concentrate the entire NCC LL1 data stream into a smaller number of LL1 modules simplifying the data cross-stitching required for jet cluster trigger algorithms. This would only be possible by using high-speed copper serial links between the detector front end readout modules and the LL1 electronics which are inherently short-range - thus requiring the LL1 electronics to be located in the detector hall.

The LL1 system would provide a set of photon triggers and jet cluster triggers based on the 2x2 trigger tiles where both sets of algorithms would use information from neighboring trigger tiles and the NCC depth information to provide clean photon triggers. Detailed simulations of the performance of the NCC LL1 system are underway. The reduced bit output of the NCC LL1 trigger, in the form of a set of bits indicating satisfied algorithms, would be transmitted to the GL1 system over optical fiber.

PERFORMANCE

The four panels in the Fig. 7 illustrate different aspects of the NCC design and performance directly related to the PHENIX experimental goals. The top right panel is the NCC photon energy resolution (in GeV) plotted as function of $\sqrt{E}$. The resolution is a linear function of $\sqrt{E}$ with a 20% slope up to the energies of a few tens of GeV and slightly degraded compared to this function when energy leakage to the coarse hadronic compartment becomes substantial.

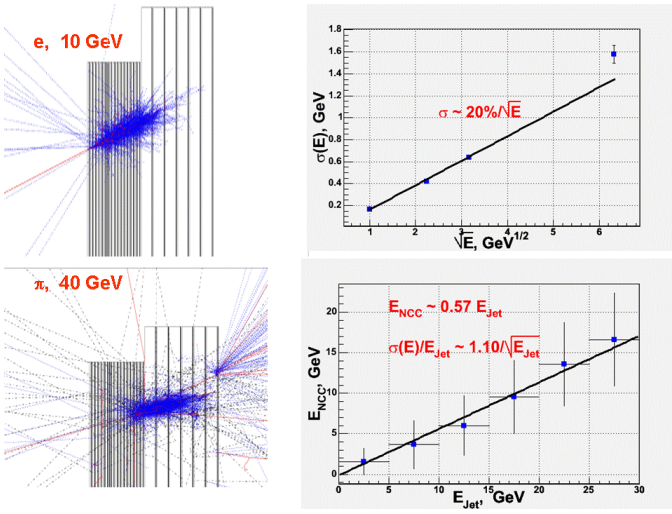

Fig. 7. NCC performance for electromagnetic shower and jet energy measurements.

Most of the electromagnetic energy stays in the electromagnetic compartments, the depth and position of those compartments with respect to shower profile are chosen to insure the linear dependence of the energy deposited in the downstream electromagnetic compartment on the momentum of the impinging photon. (A trigger on electromagnetic energy can be based upon hits in the first compartment only).. Comparable lateral and longitudinal dimensions of the individual sub towers in electromagnetic and hadronic compartments allow for independent position measurements in every compartment and provide some degree of pointing capabilities. Geometrically very shallow subtowers help to minimize the underlying event contribution to the measured shower energy and improve two shower separation at extreme impact angles.

Space constraints limit the total depth of calorimeter to less then 2 Labs resulting in a substantial leakage of hadronic energy into the iron of the magnet pole backing the NCC. Comparison between energies of simulated jets and those seen in NCC (sum of energies scaled by respective sampling fractions) presented in the bottom right panel in Fig. 7 shows that jet energy measurements in this calorimeter are certainly limited by fluctuations in the amount of energy lost from leakage section. Preliminary estimates predict a jet energy resolution of about 110%/√E (Fig.7). While jet energy measurements will have only limited validity, the fine lateral segmentation of the calorimeter will allow the measurement of the jet space vector with resolution fully satisfactory to reconstruct the kinematics of hard scattering.

It is worth noting that a tungsten calorimeter with a shallow electromagnetic compartment will have little hadronic energy deposited in that compartment. Electromagnetic showers within a jet cone identified by the energy pattern in the first two compartments will be used to improve jet energy resolution and to study modifications to jet fragmentation in nuclear matter.

A difference in the shower penetration and longitudinal shower shape serve a basis for hadron suppression and allow the NCC to be used as standalone photon identifier (Fig. 8).

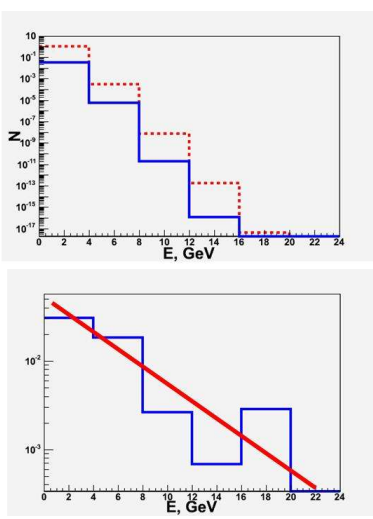

Fig. 8. Momentum spectrum of charged pions hitting the NCC in hard scattering pp events at √s=200 GeV simulated with PYTHIA (top panel – dotted histogram) and the energy spectrum of hadronic showers passing the shower shape test applicable to electromagnetic showers (top panel – solid histogram). Testing is based solely upon longitudinal shower shape. The ratio of the two histograms indicating the level of suppression of charged hadrons using this method is shown in the panel at the bottom.

The momentum spectrum of hadrons in this picture (bottom histogram) was normalized to the average hadron multiplicity in NCC. Consequently the solid histogram on the top panel can be interpreted as an expected per event multiplicity of fake electromagnetic showers. This value is to be compared to the corresponding numbers for direct photons. The latter can be estimated from PHENIX published data on $\pi 0$ and direct photon production in pp interactions at 200 GeV [8,9]. In the pT range above 6 GeV/c where direct photon yield exceeds 10% of the $\pi 0$ yield (~5% of the charge hadron yield) fake electromagnetic showers are less then 1% of the total hadronic yield corresponding to direct photon to fake electromagnetic showers ratio better then 10%.

Since the NCC is located only 40cm from the nominal collision vertex, the job of separating single isolated photons from overlapping photons from $\pi 0$ decays is extremely challenging. The NCC design incorporates a $\gamma/\pi 0$ identifier built of Si strips 0.5 mm wide. Simulations show that two shower separation will be possible down to the impact point separation ~2 mm corresponding to $\pi 0$ momenta ~ 15 GeV. We will explore all potential algorithms for reducing the $\pi 0$ background to single photons such as independent handling of data in all three longitudinal sections to control the lateral shower shape. However we do not expect further significant improvements to two shower separation unless the granularity is substantially increased.

Acknowledgement

We thank our PHENIX collaborators for the support and encouragement of the proposed upgrade and fruitful discussions.

References

PHENIX Conceptual Design Report, PX20, BNL48922 internal report, 1993

The Relativistic Heavy Ion Collider Project: RHIC and its Detectors, Edited by M. Harrison, T. Ludlam and S. Ozaki, NIMA499 , Issues 2-3, 235-880, 2003

Seto, R., Future measurements at RHIC, Proceedings of Workshop on Nuclear Dynamics, Bahamas, January 2002, World Scientific 2002, nucl-ex/ 0204003.

L. McLerran, R. Venugopalan, Phys. Rev. D49, 1994, 2233; L. McLerran, R. Venugopalan, Phys. Rev. D49, 1994, 3352; L. McLerran, R. Venugopalan, Phys. Rev. D50, 1994, 2225; see also E. Iancu, A. Leonidov, and L. McLerran hep-ph/0202270 and hep-ph/0202025 for a nice review of the saturation and RHIC physics.

I. Golutvin et al.. A Silicon Hadron Calorimeter module operated in a strong magnetic field with VLSI read out for LHC, CERN-DRDC-91-54, CERN-DRDC-P-34, Jan 1992

J.H. Adams et al., The Silicon Matrix as a Charge Detector for the ATIC Experiment, Instrum.Exp.Tech. 44, 455-461, 2001, Prib.Tekh.Eksp. 2001 N4, 38-44, 2001

V. Bonvicini et al., New concepts in silicon calorimetry for space experiments, NIM.A518:186-187,2004

S.S.Adler et al., Midrapidity Neutral-Pion Production in Proton-Proton Collisions at $\sqrt{s}$=200 GeV, Phys. Rev. Lett. 91, 241803, 2003

S.S.Adler et al., Mid-Rapidity Direct-Photon Production in p+p Collisions at sqrt(s) = 200 GeV, hep-ex/0502006, 2005

SPARES

Off-line, the early sampling of the showers and the good position resolution of the detector will provide additional means for identifying electrons

2.5.2 Stripixel sensors and stripixel readout layers

One of the major tasks NCC will need to complete is to study direct photon production in events with correlated photon-jet in the final state resulting from compton scattering of soft gluon on a quark. This is probably he most revered process as concerns our ability to access the partonic evolution in the initial state leading to sQGP formation. The background to this process are the double-jet final states with one fragmenting into leading p0 faking single photon due to shower overlaps. In the detector bilt of composite material with Molier radius rM ~18 mm and characteristic slope of the shower core ~0.2 rM = 4 mm, the clear separation of the maxima due to two photons with close energies is possible down to a similar value of d~0.2 rM (Fig. 17).
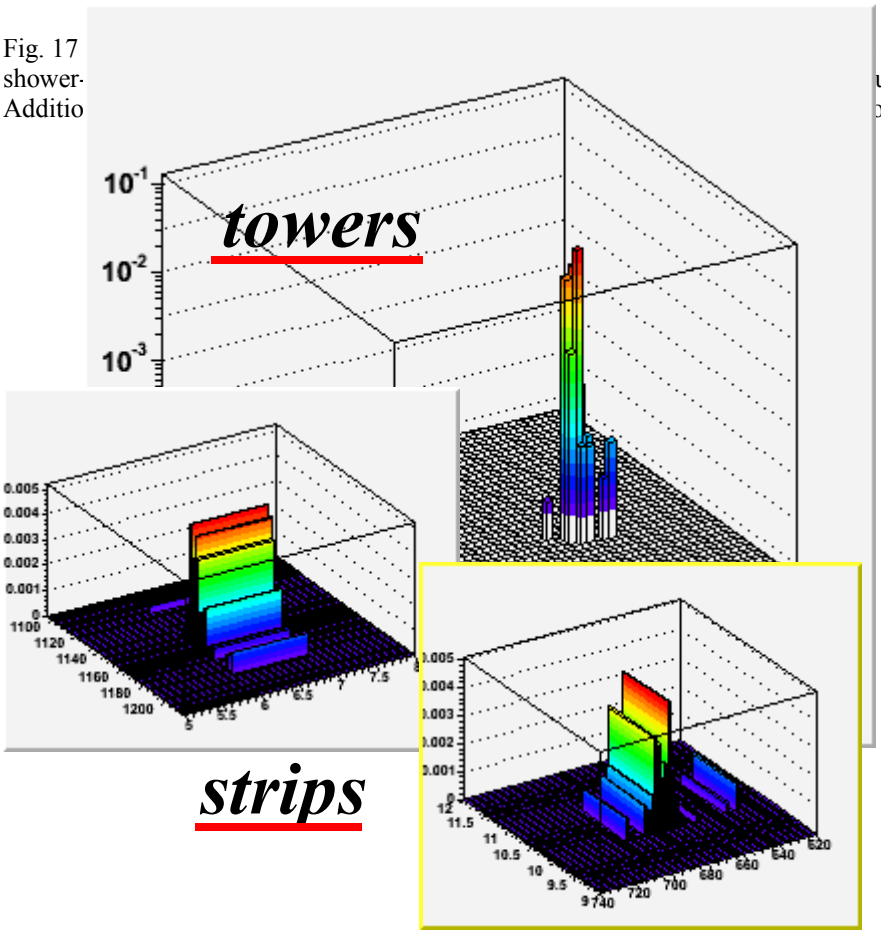
Fig. 17 and in the strips of the detector located at a shower- ut clearly separated in shower max detector. Additio ower.